β''-Al$_2$O$_3$ Single-Crystal Films and their Optical Properties

CHU KUN KUO & PATRICK S. NICHOLSON

Ceramic Engineering Research Group, Department of Materials Science and Engineering, McMaster University,
Hamilton, Ontario, Canada L8S 4L7

Abstract. The development of large-area, Na-β''-Al$_2$O$_3$ single-crystal films on sapphire substrates via vapor reaction is reported. The films form at the expense of the sapphire which reacts with the alkali-vapors generated from mixed (Na,Li)-β''-Al$_2$O$_3$ powders occupying the same space as the sapphire. A number of β''-Al$_2$O$_3$ single-crystal, large area isomorphs have been synthesized via ion exchange and their refraction and luminescence properties are reported. Patterned luminescence has been achieved in Cu$^+$-doped single-crystal films using an electrochemical cell with β''-Al$_2$O$_3$ electrolyte separator between aqueous-solution electrodes. Ag$^+$ ions are injected into the β''-Al$_2$O$_3$ electrolyte and Na$^+$ expelled. The distribution of luminescent and environment ions is controlled by electrical charge and the chemical potential of the ions in the solution electrodes.

Keywords: β''-alumina, single crystal film, molar refractivity, luminescence, luminescence patterning

I. Introduction

β''-Al$_2$O$_3$ has interesting optical properties [1–3]. The reasons are: (1) Doped ions are exchangeable at low temperatures favorable for incorporation of dopants unstable at higher temperatures, (2) The possibility of high doping levels (up to several percent), as the open structure tolerates dimensional change without lattice damage and (3), $\beta''(\beta)$-Al$_2$O$_3$ is a fast, ion-conductor. Optically-active ions doped onto the conduction plane are mobile and weakly bonded. Their optical emission properties are sensitive to variations of local crystal and electrical fields.

The potential application of β''-Al$_2$O$_3$ crystals to optics has been studied since the nineteen eighties. Cu$^+$-β''-Al$_2$O$_3$ exhibits broad-band luminescence determined by codopant ions [4,5]. This suggested application to tuneable, solid-state phosphors and lasers. Optical memory function was also reported for the Cu$^+$-doped β''-Al$_2$O$_3$ crystals [6], and Nd-β''-Al$_2$O$_3$ was used for lasers [7] and degenerate four-wave mixers [8].

Large-area Na-β''-Al$_2$O$_3$ single-crystal films have been successfully grown on sapphire substrates and their ion transport and exchange properties demonstrated. These films are of interest for large-area, planar optical devices. This paper reviews the synthesis and optical properties of these single-crystal films.

II. Na-β''-Al$_2$O$_3$, Single-Crystal-Film Preparation

Na-β''-Al$_2$O$_3$ single-crystal films are grown on highly-polished, (001)-cut sapphire substrates [9,10]. The substrate, in a covered platinum-, or β''-Al$_2$O$_3$ coated, alumina-crucible, is heated to 1200°–1350°C for tens of hours in the vapor of Na- and Li-β''-Al$_2$O$_3$ mixed powders. The alkali partial-pressure is appropriate for β''- or β-Al$_2$O$_3$ formation but not for sodium aluminate. The resulting single-crystal films are $\leq 40\,\mu m$ thick and transparent (Fig. 1). The rhombohedral-symmetric patterns are characteristic.

X-ray diffraction shows overlapped β''- and α-Al$_2$O$_3$ patterns (Fig. 2). The (*00l*) peaks of the β''-Al$_2$O$_3$ and α-Al$_2$O$_3$ indicate single-crystal film/ substrate $\langle 001 \rangle$ epitaxial alignment, i.e., the c-axes
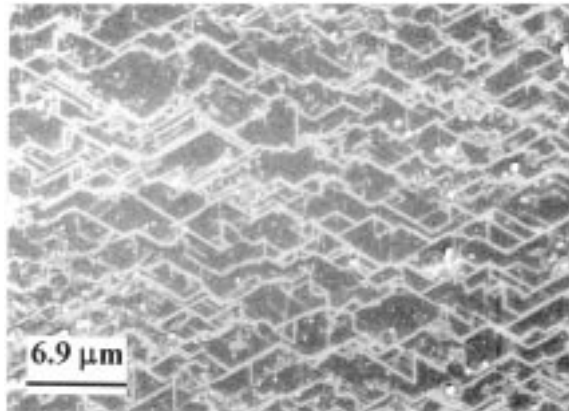
Fig. 1. SEM of Na-β''-Al$_2$O$_3$ single-crystal film grown from sapphire substrate.

coincide. X-ray precession determined that the film/substrate a-axes differ by $\pi/6$ [11] (Fig. 3). These crystallographic relationships suggest the β''-Al$_2$O$_3$ crystal grows on the close-packed oxygen layer of the sapphire.

The time dependence of film thickness is satisfactorily described by a diffusion equation with:

$$D(\text{cm}^2/\text{s}) = 1.72 \times 10^{13}(\text{cm}^2/\text{s})$$
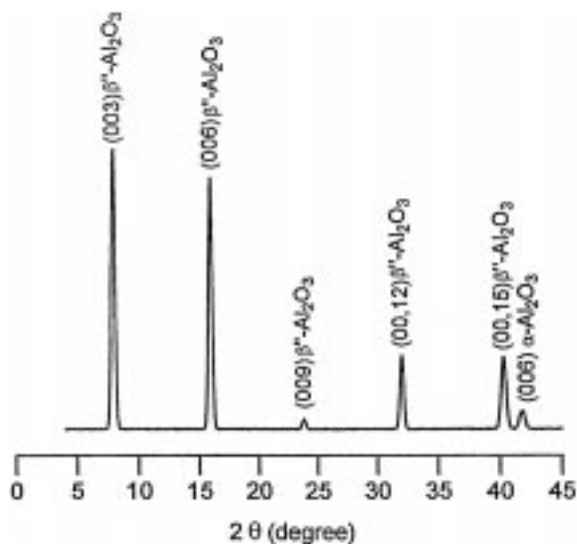
$$\exp(-718.4(\text{kJ/mole})/RT)$$

Fig. 2. The X-ray diffraction pattern of Na-β''-Al$_2$O$_3$ single-crystal film grown on sapphire substrate showing *(00l)* peaks.
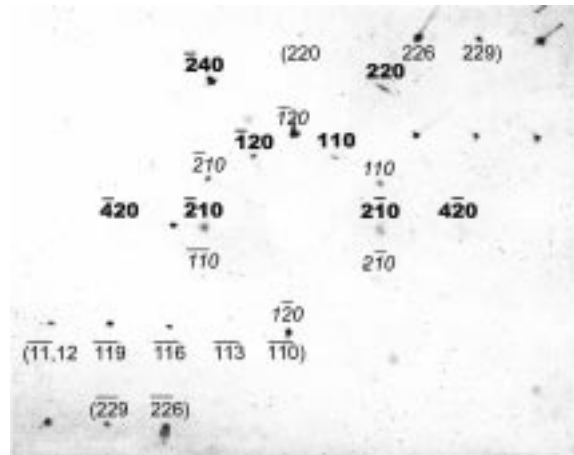

Fig. 3. An X-ray precession photograph showing overlapped diffractions $\langle 110 \rangle$ (included in brackets) and $\langle 001 \rangle$ (regular letter) of α-Al$_2$O$_3$ and $\langle 001 \rangle$ (bold letter) of Na-β''-Al$_2$O$_3$. Indices are labeled only on selected diffraction points for the sake of clarity.

Weight change and rate-of-process results suggest vapor-substrate reaction occurs rather than chemical vapor deposition. Reactions between alkali-rich vapor and α-Al$_2$O$_3$ are thermodynamically favorable. The growth of Na-β''- or β-Al$_2$O$_3$ at α-Al$_2$O$_3$/ sodium aluminate interfaces was reported controlled by oxygen [12] or Na-Al counter-diffusion [13] with activation energy 189 and 470 kJ/mole, respectively. The suggestion of cation counter diffusion was supported by the production of β''- and β-Al$_2$O$_3$ in two reaction zones. High diffusion rates of oxygen were found at grain boundaries [14,15], and the decreased activation energies for the ceramic systems are associated therewith. If Al^{3+} transport to the surface governs the process of β''-Al$_2$O$_3$ film growth, it must involve oxygen layer disintegration and reconstruction. Metastable sodium aluminate might be expected due to the high sodium concentration at the growing surface and the slow reactant diffusion rate thereto. No such phase was identified in the film.

Furthermore, the activation energy is similar to that for oxygen diffusion in α-Al$_2$O$_3$ single crystals [16–18]. This suggests oxygen transport occurs across the close-packed oxygen spinel block and the sapphire-to-β''-Al$_2$O$_3$ reaction is controlled by oxygen diffusion along the c-axis.

III. Ion Exchange of β''-Al$_2$O$_3$ Isomorphs

The Na-β''-Al$_2$O$_3$ films [19] did not crack or fragment as the sodium was replaced by ions of different radii (lithium, potassium, barium). The process induces trivial dimension change at the sapphire/film interface, but a significant one in the c-direction. As the film is single crystal, the latter is free to occur. Typical ion exchange conditions for the Na-β''-Al$_2$O$_3$ films are listed in Table 1.

Ion exchange in fused salts was satisfactory but it was difficult to control ion distribution via conventional cell-charging or surface-masking techniques because the requisite high temperatures caused sealing and corrosion problems. An aqueous approach [20] was therefore developed. Silver nitrate solution was employed for Ag$^+$-Na$^+$ exchange $< 100°C$. Weight gain and X-ray diffraction tracked the exchange fractions (Fig. 4). The X-ray diffraction patterns show increases in the (009) and (00,12) reflection intensities versus those of (003) and (006). Greater than 80% exchange was attained $\approx 50\,h$ and was accelerated by an imposed dc field.

IV. Optical-Properties

1. Refractive Properties and Polarizability of Cations and Oxide Anions

Na-β''-Al$_2$O$_3$ is strongly-anisotropic and strongly-birefringent. The refractive indices and birefringence vary with the nature and concentration of the exchanged ions [21,22]. The molar refractivity of
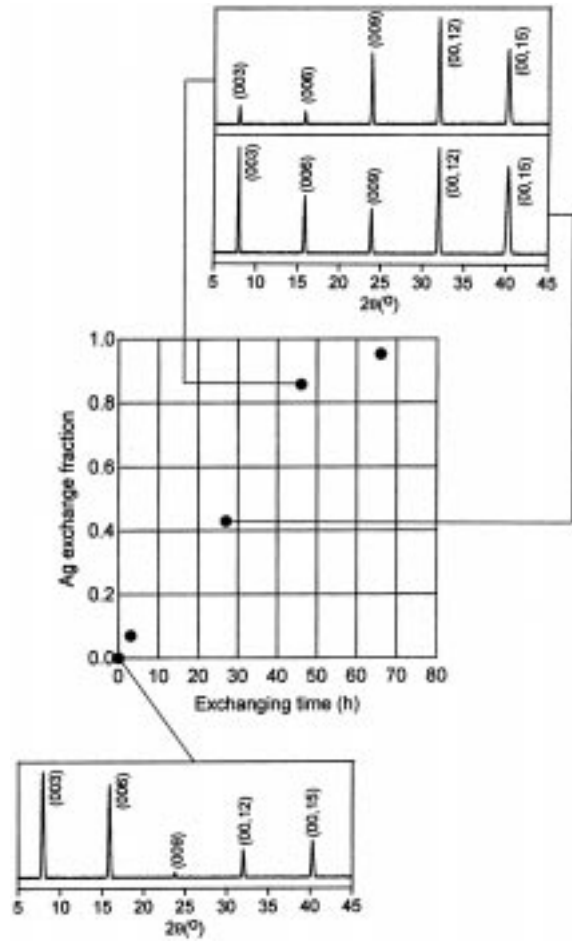
Fig. 4. The ion exchange of Na-β''-Al$_2$O$_3$ in AgNO$_3$ aqueous solution at 92°C; the X-ray diffraction pattern at 0.00, 0.43 and 0.86 exchange fractions inserted.

Table 1. Conditions for ion exchange and doping in β''-Al$_2$O$_3$ single-crystal films

Starting phase	Medium	Temperature (°C)	Time (h)
Ag-β''-Al$_2$O$_3$	LiCl	650	10.5
Na-β''-Al$_2$O$_3$	CaCl2	800	24
Na-β''-Al$_2$O$_3$	KNO$_3$	405	87
Na-β''-Al$_2$O$_3$	AgNO$_3$	270	46
Na-β''-Al$_2$O$_3$	AgNO$_3$	92	65
Na-β''-Al$_2$O$_3$	0.75CuCl-0.25NaCl	410–450	2–4
Na-β''-Al$_2$O$_3$	0.70CuCl-0.30KCl	420–470	2–4
Na-β''-Al$_2$O$_3$	0.80CuCl-0.20LiCl	470	3–6
Na-β''-Al$_2$O$_3$	0.67CuCl-0.33RbCl	450	4–6
Na-β''-Al$_2$O$_3$	0.936CuCl-0.064CaCl$_2$	485	7
Na-β''-Al$_2$O$_3$	0.70CuCl-0.30BaCl$_2$	570	5

the β''- and β-Al_2O_3 isomorphs obeys the additive rule of oxide components [21]. Refractive indices measured on the single-crystal films are listed in Table 2. The Lorentz-Lorenz formula was used for molar refractivity via the molar volume derived from the lattice constants. The refractivity of the basic-oxide component was estimated by subtracting that of γ-Al_2O_3 from the total refractivity value. The refractivity for the Al_2O_3 component was taken to be $11.33\,cm^3$. Refractivity values for bulk β''- and β-Al_2O_3 crystals and α- and γ-Al_2O_3 are also included in Table 2.

The polarizability [23,24] of the oxide components involved was evaluated using;

$$\alpha = 3MR/4\pi N_A$$

$$MR_{\beta''-Al2O3} = \Sigma MR_{oxide} = \Sigma MR_+ + \Sigma MR_-$$

$$\alpha_+ = 3MR_+/4\pi N_A, \alpha_- = 3MR_-/4\pi N_A$$

where MR is the molar refractivity, α the polarizability of the ion, N_A Avogadro's number, and $+$ and $-$ indicate the cationic and anionic species. The polarizability for cationic and oxide ions was based on the measured molar refractivity correlated to oxide ionicity [25]. The low oxygen polarizability for the

aluminum-oxygen bond is due to the strong polarising power of the trivalent Al^{3+} which increases the proximity of the valence electrons shared with the oxygen. The conducting cations have low field strength so their valence electrons are less attracted thereto thus increasing the oxide-ion polarizability.

2. Luminescence Spectroscopy of Cu^+-Doped Na-β''-Al_2O_3 Single-Crystal Films

Active ions locate on the two available sites of the β''-Al_2O_3 conduction planes, i.e., the four-coordinated, Beevers-Ross and the eight-coordinated, mO sites. The occupation distribution depends on the ion size and polarizability factors. The occupation ratio Na(Beevers-Ross)/Na(mO) for Li-stabilized Na-β''-Al_2O_3 is 0.36–0.44 [26].

Figure 5 shows the luminescence spectrum for Cu^+-doped and ion-exchanged films of Na-β''-Al_2O_3. The emission bands are listed in Table 3. The Cu^+ ion responsible for fluorescence undergoes the transition, $3d^94s^1 \rightarrow 3d^{10}$. As in bulk crystals, the two major peaks observed at 440 and 530 nm, corresponding to blue and green emission, are attributed to Cu^+ ions on mO sites and Cu^+-Cu^+

Table 2. Optical refractivity of $\beta''(\beta)$-Al_2O_3 isomorphs and the polarisability of ions derived from the refractivity[1*]

Composition	$a_o(Å)$	$c_o(Å)$	n_o	n_e	MR	$MR_{basic\ oxide}$(ionicity)	α_{cation}	$\alpha_{oxygen\ anion}$
$Na_{1.6}Li_{0.3}Al_{10.7}O_{17}$	5.61	33.565	1.687	1.637	68.6	8.95(0.922)	0.192	2.79
$Li_{1.6}Li_{0.3}Al_{10.7}O_{17}$	5.605	33.67	1.662	1.627	67.1	7.05(0.895)	0.069	2.62
$K_{1.6}Li_{0.3}Al_{10.7}O_{17}$	5.60	34.126	1.697	1.642	70.2	10.92(0.919)	0.647	2.67
$Ag_{1.6}Li_{0.3}Al_{10.7}O_{17}$	5.604	33.46						
$Ca_{0.8}Li_{0.3}Al_{10.7}O_{17}$	5.607	33.47	1.702	1.672	70.1	9.14(0.939)	0.594	2.97
$Na_{2.58}Al_{21.81}O_{34}$[2*]	5.594	22.53	1.6655	1.6254	134.5	8.46(0.883)	0.21	2.66
$Na_{1.67}Mg_{0.67}Al_{10.33}O_{17}$[3*]	5.61	33.54	1.673	1.637	67.8	7.52		
$Ca_{0.835}Mg_{0.67}Al_{10.33}O_{17}$[3*]	5.613	33.27	1.681	1.655	68.3	8.04(0.857)	0.68	2.59
$Ba_{0.835}Mg_{0.67}Al_{10.33}O_{17}$[3*]	5.619	34.084	1.687	1.682	71.2	11.49(0.889)	1.98	2.66
α-Al_2O_3[4*]	4.751	12.991	1.7686	1.7604	10.55		0.309	1.19
γ-Al_2O_3[4*]	7.9		1.696		11.31		0.253	1.33

[1*]MR = molar refractivity (cm^3); α = polarizability ($Å^3$); the α_{cation} and $\alpha_{oxygen\ anion}$ assigned polarizabilities of the cation and O^{2-} in the basic oxide of β''- and β''-Al_2O_3, and those to Al^{3+} and O^{2-} in α- and γ-Al_2O_3.

[2*]C. R. Peters, M. Bettman, J. W. Moore and M. D. Glick, "Refinement of the Structure of Sodium β-Alumina," *Acta Crystallogr.*, B27, 1826–1834 (1971).

[3*]G. C. Farrington and B. Dunn, "Divalent Beta-Aluminas: High Conductivity Solid Electrolytes for Divalent Cations," *Solid State Ionics*, 7, 267–281 (1982); [22].

[4*]JCPDS (Joint Committee on Powder Diffraction Standards)—ICDD (International Center for Diffraction Data) Powder Diffraction File No's. 10-173 and 10-425 (1988); A. N. Winchell and H. Winchell, *The Microscopical Characters of Artificial Inorganic Solid Substances: Optical Properties of Artificial Minerals,* (Academic Press, New York, 1964), pp. 59–60.
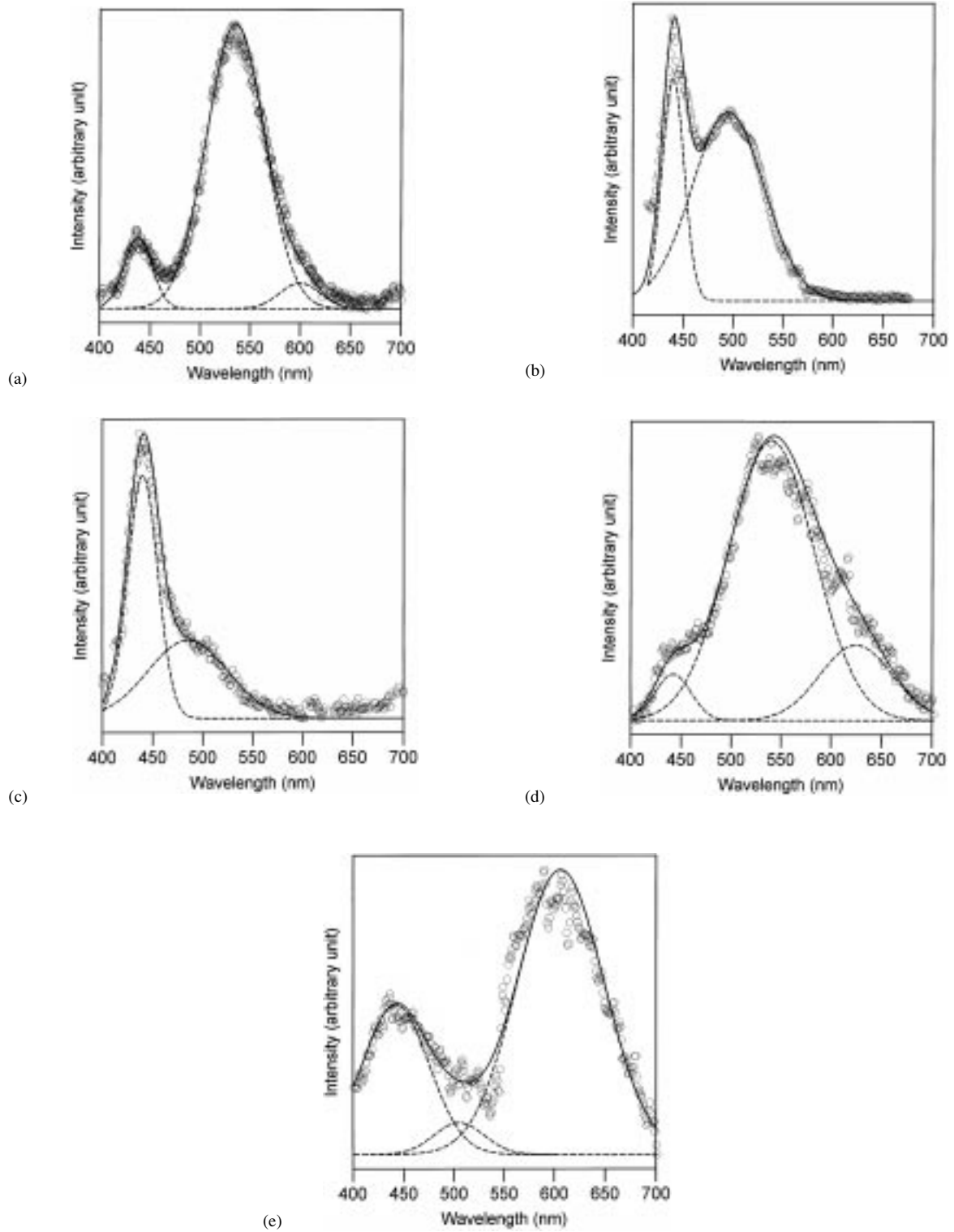
(a)

(b)

(c)

(d)

(e)

Fig. 5. Luminescence spectrum of β''-Al$_2$O$_3$ isomorph single-crystal films: (a) Cu$^+$: Na-β''-Al$_2$O$_3$, (b) Cu$^+$: K-β''-Al$_2$O$_3$, (c) Cu$^+$: Ba-β''-Al$_2$O$_3$, (d) and (e) the green and purple luminescent part in the luminescence-patterned Cu$^+$-doped β''-Al$_2$O$_3$ sample.

Table 3. Emission bands of the Cu^+-doped β''-Al_2O_3 spectrum

	Emission (fraction)		
	Blue	Green	Red
Na^+	438(0.100)	535(0.847)	600(0.053)
K^+	440(0.266)	495(0.734)	
Ba^{2+}	440(0.539)	485(0.461)	
Na^+*	442(0.053)	540(0.776)	625(0.172)
Ag^+*	442(0.255)	505(0.046)	606(0.699)

*In the luminescence-patterned sample.

dimers [5]. In addition, a minor peak was observed ≈ 600 nm (red) for Cu^+-doped Na-β''-Al_2O_3 single-crystal films. This was not reported for the bulk crystal. Cu^+-activated red luminescence was however detected for Ag-β''-Al_2O_3 bulk crystal [4], $LaCuO_2$ [27] and a number of the complex compounds [28–31]. In the latter cases, emission was explained by metal-ligand charge transfer or by the $3d^9 4s^1$ excited state being strongly modified by copper–copper interactions.

The blue luminescence remains at 440 nm and is enhanced when K^+ and Ba^{2+} replace Na^+ in the host lattice. This is due to the increased polarizability of K^+ and Ba^{2+} which reduces the interaction with O^{2-} and increases the $Cu^+ - O^{2-}$ interaction. The latter suppresses the tendency to form Cu^+ clusters. The green luminescence (530 nm) is more sensitive to ion replacement and varies between 535 nm (Na-β''-Al_2O_3) and 485 nm (Ba-β''-Al_2O_3). This shift is associated with the increased polarizability of the matrix cations and the consequent decrease of covalency of the host lattice (as observed for most luminescent ions). The red emission band was enhanced in the Ag/Na-β''-Al_2O_3 host as expected via the interpretation that the energy of the excitation state is lowered by lattice covalency. Moreover, Ag^+ has a non-inert-gas electron-shell configuration and this could increase the partial covalency of the conducting sublattice thus promoting Cu^+-Cu^+ cluster formation.

3. Luminescence Patterning of $\beta''-Al_2O_3$ Single-Crystal, Large-Area Films

The following electrochemical cell [32] was used to introduce a controlled ion-distribution (and thus

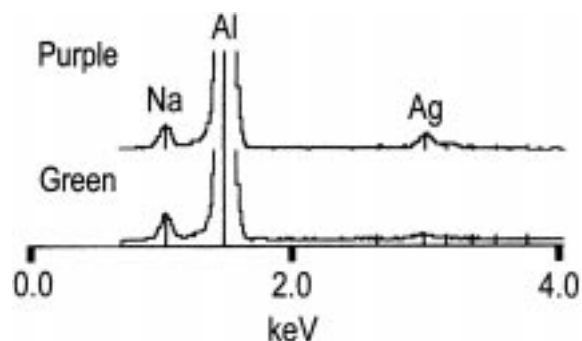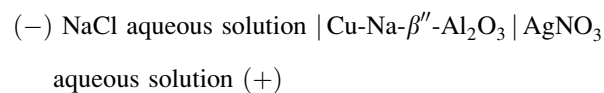*Fig. 6.* EDX spectrum of luminescence-patterned Cu^+-doped-β''-Al_2O_3 sample showing Na and Ag contents in the green and purple luminescent parts.

luminescence patterns) in a Na-β''-Al_2O_3 single-crystal film:

$(-)$ NaCl aqueous solution $|$ Cu-Na-β''-Al_2O_3 $|$ AgNO$_3$

   aqueous solution $(+)$

Two co-axial glass tubes held the ion-exchange solutions (NaCl and $AgNO_3$) with the Cu^+-doped Na-β''-Al_2O_3 single-crystal film as separator. The cell was electrically charged < 10 V, at 78°–95°C for ≤ 10 h so Ag^+ passed from the $AgNO_3$ to the NaCl through the Cu-Na-β''-Al_2O_3. As a result, silver ions entered the right part of the β''-Al_2O_3 and sodium exited the left.

After charging, the green luminescence of Cu/Na-β''-Al_2O_3 changed to purple on the right but remained unchanged on the left. Two-luminescence pieces were obtained (Fig. 5(d) and (e)). EDX analysis (Fig. 6) shows the Na^+/Ag^+ content of the two luminescent domains.

The sharp boundary between the green-purple regions is considered due to the gradient of Ag^+ and Na^+ activities in the solutions. The green luminescence is from Cu^+ activated Na-β''-Al_2O_3, the purple from Ag/Na-β''-Al_2O_3.

V.   Summary

1. Na-β''-Al_2O_3 single-crystal films were grown on (001) sapphire substrates by heating the latter in a controlled alkali-containing atmosphere. The epitaxial crystallographic relations between the single-crystal film and the sapphire sub-

strate are; c-axis$_{Na-\beta''-Al2O3}\|$(c-axis$_{sapphire}$ and a-axis$_{\beta''-Al2O3} \wedge$ a-axis$_{sapphire} = \pi/6$.

2. The refraction and luminescence properties of the β''-Al$_2$O$_3$ large-area single-crystal films are given. The molar refraction values measured for the β''-Al$_2$O$_3$ isomorphs are used to calculate the polarizability of ions, i.e., for the oxygen anion in ''Al$_2$O$_3$'', it is 1.33 cm^3 and the basic-oxide components are 2.59–2.97 cm^3.

3. The luminescence of Cu$^+$-doped β''-Al$_2$O$_3$ single-crystal film is interpreted in terms of the host environment and the polarisability of the ions in the conducting sublattice. The luminescence of a Na/Ag-β''-Al$_2$O$_3$ single crystal film was patterned by electric-field-assisted ion-exchange. The distribution of the green(Cu-Na)/purple(Cu-Ag) luminescence is determined by the chemical potential values of the Ag$^+$ and Na$^+$ in the electrode compartments of the ion-patterning cell.

References

1. G.C. Farrington, B. Dunn, and J.O. Thomas, *Appl. Phys.*, **A32**, 159 (1983).
2. B. Dunn and G.C. Farrington, *Solid State Ionics*, **18/19**, 31 (1986).
3. C.K. Kuo and P.S. Nicholson, *J. Canadian Ceramic Soc.*, **65**, 139 (1996).
4. J.D. Barrie, B. Dunn, O.M. Stafsudd, and P. Nelson, *J. Luminescence*, **37**, 303 (1987).
5. J.D. Barrie, B. Dunn, G. Hollingsworth, and J.I. Zink, *J. Phys. Chem.*, **93**, 3958 (1989).
6. G. Hollingsworth, J.D. Barrie, B. Dunn, and J.I. Zink, *J. Amer. Chem. Soc.*, **110**, 6569 (1988).
7. M. Jansen, A. Alfrey, O.M. Stafsudd, B. Dunn, D.L. Yang, and G.C. Farrington, *Optics Lett.*, **9**, 119 (1984).
8. R.W. Boyd, M.T. Gruneisen, P. Narum, D.J. Simkin, B. Dunn, and D.L. Yang, *Optics Lett.*, **11**, 162 (1986).
9. A. Tan, C.K. Kuo, and P.S. Nicholson, *Solid State Ionics*, **67**, 131 (1993).
10. C.K. Kuo and P.S. Nicholson, *Solid State Ionics*, **67**, 157 (1993).
11. C.K. Kuo and P.S. Nicholson, *Solid State Ionics*, **82**, 173 (1995).
12. J.D. Hodge, *J. Amer. Ceram. Soc.*, **66**, C154 (1983).
13. A. Ya. Neiman, I.E. Tigieva, L.A. Litvinov, and V.V. Pishchik, *Russ. J. Inorg. Chem.*, **31**, 490 (1986).
14. R.O. Ansell, A. Gilmour, and R.J. Cole, *J. Electroanal. Chem.*, **244**, 123 (1988).
15. L.C. De Jonghe and A. Buechele, *J. Mater. Sci.*, **17**, 885 (1982).
16. Y. Oishi and W.D. Kingery, *J. Chem. Phys.*, **33**, 480 (1960).
17. D.J. Reed and B.J. Wuensch, *J. Amer. Ceram. Soc.*, **63**, 88 (1980).
18. H. Haneda and C. Monty, *J. Amer. Ceram. Soc.*, **72**, 1153 (1989).
19. C.K. Kuo and P.S. Nicholson, *Solid State Ionics*, **69**, 163 (1994).
20. C.K. Kuo and P.S. Nicholson, *Solid State Ionics*, **91**, 81 (1996).
21. C.K. Kuo and P.S. Nicholson, *Solid State Ionics*, **58**, 173 (1992).
22. S.C. Adams, B. Dunn, and O.M. Stafsudd, *Optics Lett.*, **13**, 1072 (1988).
23. J.R. Tessman, A.H. Kahn, and W. Shockley, *Physical Review*, **92**, 890 (1953).
24. H.W. Jaffe, *Crystal Chemistry and Refractivity* (Cambridge University Press, Cambridge, 1988).
25. Y.Y. Guo, C.K. Kuo, and P.S. Nicholson, *Solid State Ionics*, **110**, 327 (1998).
26. J.D. Jorgensen, F.J. Rotella, and W.L. Roth, *Solid State Ionics*, **5**, 143 (1981).
27. J.-P. Doumerc, C. Parent, Z.J. Chao, G. Le Flem, and A. Ammar, *C. R. Acad. Sci., Paris, Ser. II*, **306**, 1431 (1988).
28. A. Vogler and H. Kunkely, *J. Amer. Chem. Soc.*, **108**, 7211 (1986).
29. A.K.I. Gushurst, D.R. McMillin, C.O. Dietrich-Buchecker, and J.-P. Sauvage, *Inorg. Chem.*, **28**, 4070 (1989).
30. K.R. Kyle, C.K. Ryu, J.A. DiBenedetto, and P.C. Ford, *J. Amer. Chem. Soc.*, **113**, 2954 (1991).
31. D.M. Knotter, G. Blasse, J.P.M. van Vliet, and G. van Koten, *Inorg. Chem.*, **31**, 2196 (1992).
32. Y. Shimizu, C.K. Kuo, and P.S. Nicholson, *Solid State Ionics*, **110**, 69 (1998).